

Coulomb-Modified Fano Resonance in a One-Lead Quantum Dot

A. C. Johnson,¹ C. M. Marcus,¹ M. P. Hanson,² and A. C. Gossard²

¹*Department of Physics, Harvard University, Cambridge, Massachusetts 02138, USA*

²*Department of Materials, University of California, Santa Barbara, California 93106, USA*

(Received 22 December 2003; published 3 September 2004)

We investigate a tunable Fano interferometer consisting of a quantum dot coupled via tunneling to a one-dimensional channel. In addition to Fano resonance, the channel shows strong Coulomb response to the dot, with a single electron modulating channel conductance by factors up to 100. Where these effects coexist, line shapes with up to four extrema are found. A model of Coulomb-modified Fano resonance is developed and gives excellent agreement with experiment.

DOI: 10.1103/PhysRevLett.93.106803

PACS numbers: 73.63.Kv, 73.23.Hk

The interplay between interference and interaction, in its many forms, is the central problem in mesoscopic physics. In bulk systems, screening reduces strong Coulomb repulsion to a weak interaction between quasiparticles, but in confined geometries, electron-electron interaction can dominate transport. The Fano effect—an interference between resonant and nonresonant processes—was proposed in the context of atomic physics [1]. More recently, Fano resonances have been seen in condensed matter systems, including surface impurities [2], quantum dots [3,4], and carbon nanotubes [5], and have generated interest as probes of phase coherence [6,7] and as spin filters [8]. These studies treat Fano resonance as a pure interference effect. If the resonant channel is a tunneling quantum dot, however, Fano resonance coexists with interaction in the form of Coulomb blockade. This coexistence leads to new transport regimes that to date have not been investigated theoretically or experimentally.

In this Letter, we present measurements of a Fano interferometer consisting of a quantum dot coupled to a one-dimensional channel. We independently control all couplings defining the resonant and nonresonant processes, allowing us to identify and investigate several regimes. With the channel partly transmitting but no tunneling to the dot, charge sensing is observed whereby channel conductance responds to charge on the dot [9]. If instead the dot-channel barrier is lowered and the channel pushed toward the dot, all transmitted electrons traverse the dot, and standard Coulomb blockade is seen. Between these lies the Coulomb-modified Fano regime, where resonant tunneling and direct transmission coincide, and Fano resonance is seen along with charge sensing. We develop a model that combines these effects and successfully describes the data. With this model, resonance parameters are extracted and used to evaluate interaction effects.

Two nominally identical devices were measured and showed similar behavior; we present data from one. The device (inset to Fig. 1) consists of a $0.5 \mu\text{m}^2$ quantum dot and a constriction, defined by Cr-Au gates on a

GaAs/Al_{0.3}Ga_{0.7}As heterostructure grown by molecular-beam epitaxy (MBE). The two-dimensional electron gas is 100 nm deep, with density $2 \times 10^{11} \text{ cm}^{-2}$ and mobility $2 \times 10^5 \text{ cm}^2/\text{Vs}$. The dot contains ~ 600 electrons and has level spacing $\Delta \sim 20 \mu\text{eV}$. The experiment was performed in a dilution refrigerator with an electron temperature of 50 mK, in a field of 0 to 200 mT perpendicular to the device plane. Conductance was measured using a lock-in amplifier with $10 \mu\text{V}$ excitation at 15.7 Hz.

Figure 1 shows conductance in the Fano regime as a function of gate voltage V_g over seven resonances. Each resonance comprises a dip and a peak similar to Fano resonance, but the noninteracting Fano line shape of Eq. (1) below fits poorly. However, a model incorporating Coulomb interaction (described below) gives quite good fits, as seen in Fig. 1.

We first discuss qualitatively the limiting regimes, as well as the intermediate Coulomb-modified Fano regime. When the channel is tuned to partially transmit one mode, but there is no conductance between channel and dot, sawtooth patterns such as Fig. 2(a) appear. These can be explained by considering a single effective gate, combining the effects of the metal gate and the dot charge, that smoothly (but not monotonically) modulates g , the

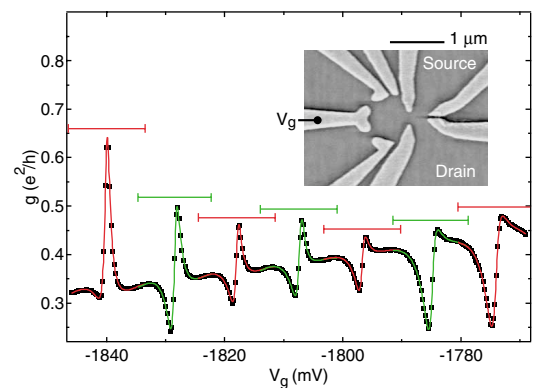


FIG. 1 (color). Channel conductance data (squares) and fits (curves) vs gate voltage V_g in the Fano regime. Bars show fitting ranges. Inset: SEM image of a similar sample, a quantum dot coupled by one lead to a conducting channel.

channel conductance. Each dot electron modifies the effective gate by a voltage V_s , which we call the *sensing voltage*. When a charge is added to the dot (as V_g is made more positive), the effective gate voltage jumps by V_s , and g jumps to the value it had at a gate voltage more negative by V_s . If g is a decreasing (increasing) function of V_g , this gives an upward (downward) jump. Thus, when the slope changes sign near -1865 mV in Fig. 2(a), the jumps change sign as well. In this device V_s is typically $\sim 80\%$ of the spacing between jumps, indicating that the channel is more sensitive to excess dot charge than to the gate directly.

The Coulomb-modified Fano regime emerges as tunneling is introduced between the dot and the channel. When charge sensing is relatively weak, such as in Fig. 1, features resembling noninteracting Fano resonance are observed. In other cases, such as Fig. 2(b), the charge sensing jump can be larger than the resonance peak. Combining this jump with the dip-peak pair of Fano resonance, one resonance can have up to four extrema.

When direct conductance is made much smaller than conductance through the dot, the direct path no longer interferes significantly with the resonant path. In this limit, we cross over to the familiar Coulomb blockade regime, yielding the simple peaks of Fig. 2(c).

Before analyzing the Fano regime in detail, we turn to features that can appear as Fano resonance but actually result from charge sensing alone. Figure 3 shows the effect of quantized dot charge on a resonance in the channel, with no tunneling between the two. Channel

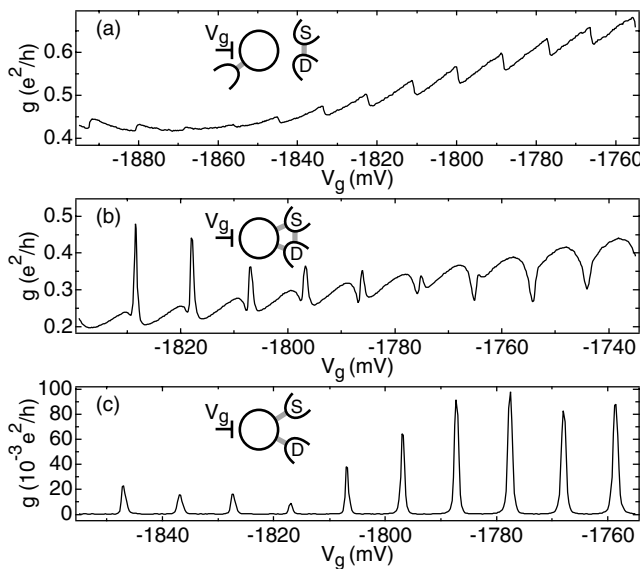


FIG. 2. Three configurations with a tunnel coupled dot. Drawings indicate tunneling paths. (a) Pure charge sensing: the dot couples capacitively to the channel and tunnels weakly to a third reservoir. (b) Fano resonance with charge sensing: tunneling between the channel and the dot interferes with direct transmission. (c) Breit-Wigner resonances: the only conducting path is through the dot.

106803-2

conductance was measured while tuning the tunnel rate from the dot to a third reservoir. When this rate is low [Fig. 3(a)], one finds smooth segments punctuated by jumps, which we identify as single tunneling events. The dotted curves are identical forms offset by $V_s = 4.0$ mV, indicating how channel resonances would appear for a dot fixed at $n = N$ or $N + 1$ electrons. If this family of curves is extended to all n , it overlays every segment of the data, though jumps from one curve to the next are irregularly spaced and move if the sweep is repeated, from which we estimate a tunneling time \hbar/Γ of order seconds.

As tunneling to the third reservoir is increased [Fig. 3(b)], jumps become periodic and repeatable, but there remains a family of evenly spaced curves onto which all of the data falls. Here the resonance is narrower, and adding one charge to the dot shifts the channel from on to far off resonance. This single-electron switch has an on/off conductance ratio of 20. Traces with still narrower resonances show ratios >100 , as in other recent reports [10]. Notice, however, the similarity of these line shapes to Fano resonance, though this is pure charge sensing.

Still greater coupling to the third reservoir yields lifetime-broadened jumps. This is the case in Fig. 3(c), where the dominant feature is a single wide resonance, modulated by weak charge quantization in the dot. This motivates an important feature of the model, that the Fano resonance and the charge sensing jump, as they result from the same process, have the same width Γ .

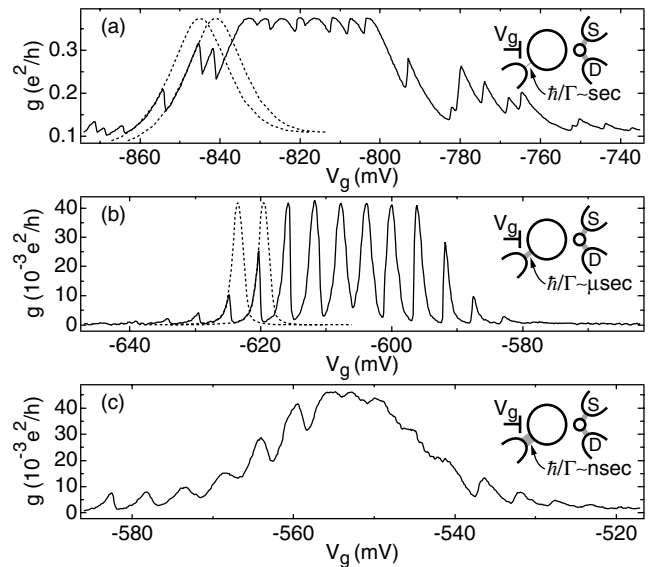


FIG. 3. Charge sensing by a channel resonance. Drawings indicate the tunneling rate to the extra lead. Dotted curves show how the full resonance would look with dot charge fixed at two consecutive values. (a) With the dot nearly isolated, jumps between these curves are sharp, erratic, and unrepeatable. (b) Increase tunneling and the jumps become periodic and repeatable. (c) With the dot nearly open, the jumps broaden and resemble an oscillation superimposed on a single, broad resonance.

106803-2

In the single-level transport regime, $kT < \Gamma < \Delta$, transmission via one discrete level produces a Breit-Wigner resonance. A transmission amplitude $t = t_0/(\varepsilon + i)$ with dimensionless detuning $\varepsilon = (E - E_0)/(\Gamma/2)$ describes an electron of energy E , a resonance at E_0 with width Γ , and peak transmission t_0 due to lead asymmetry. Conductance is proportional to the transmission probability $|t|^2$, giving a Lorentzian line shape [11]. A continuum channel can be added to the amplitude (coherently) or probability (incoherently), giving the noninteracting Fano line shape,

$$g(E) = g_{inc} + g_{coh} \frac{|\varepsilon + q|^2}{\varepsilon^2 + 1}, \quad (1)$$

where g_{coh} (g_{inc}) is the coherent (incoherent) contribution to the continuum conductance. The Fano parameter q selects from a symmetric peak ($q = \infty$) or dip ($q = 0$), or a dip to the left ($q > 0$) or right ($q < 0$) of a peak. In Fig. 1, q evolves from 2.5 to 0.6 left to right. In cases with arbitrary phase between the resonant and nonresonant paths, such as an Aharonov-Bohm ring, q is complex, which is equivalent to increasing g_{inc} . In the present context, the interfering paths enclose no area, forcing a real q . This removes ambiguity between g_{inc} and $\text{Im } q$, and constrains the Fano line shape to maximum visibility [6].

The Coulomb-modified Fano effect can be modeled by extending Eq. (1) to include nearby resonances and charge sensing effects. We write g as a sum over initial occupation n of the dot,

$$g(V_g) = \sum_n g_n(V_g) p_n(V_g). \quad (2)$$

Starting from n electrons, the only processes allowed are the addition ($n \rightarrow n + 1$) or removal ($n - 1 \rightarrow n$) of one electron. The contribution of the n -electron dot is thus

$$g_n(V_g) = g_{inc}(\tilde{V}_n) + g_{coh}(\tilde{V}_n) \times \left| 1 + \frac{q(\tilde{V}_n) - i}{\varepsilon_{n-} + i} + \frac{q(\tilde{V}_n) - i}{\varepsilon_{n+} + i} \right|^2. \quad (3)$$

The allowed resonances have detunings $\varepsilon_{n\pm} = (eV_g C_g / C_{tot} + E_{n \rightarrow n \pm 1}) / (\Gamma/2)$, including a contribution from V_g , with a lever arm given by the ratio of gate to total dot capacitance. The resonances add coherently to a direct conductance g_{coh} [12]; g_{inc} is added to account for multiple channel modes and explicit decoherence. Finally, each term is weighted by $p_n(V_g) = [\tan^{-1}(\varepsilon_{n-}) - \tan^{-1}(\varepsilon_{n+})] / \pi$, the zero-temperature probability of occupation n . This can be derived from the Friedel sum rule, which relates changes $\delta(\dots)$ in transmission phase to fractional changes in dot occupancy, $\delta[\arg(t)] = \pi \delta(\langle N \rangle) \text{ mod } \pi$, where t is the Breit-Wigner transmission or reflection amplitude [13,14].

Charge sensing enters Eq. (3) via the effective gate voltage $\tilde{V}_n = V_g - nV_s$. We expand dependences on \tilde{V}_n to first order, $q(\tilde{V}_n) = q_0 + \tilde{V}_n dq/dV_g$, and similarly for

g_{coh} and $g_{tot} = g_{inc} + g_{coh}$. The slope dg_{tot}/dV_g gives the charge-sensing sawtooth, where charges in the dot affect the potential in the channel. Nonzero dq/dV_g and dg_{coh}/dV_g subtly change the line shape near resonance, and reveal how the potential seen by a charge in resonance depends self-consistently on its probability to be in the dot. As nearby resonances are generally similar in line shape, the model assumes they obey the same linear expressions in influencing the tails of the resonance being fitted. This permits fitting overlapping ranges as shown in Fig. 1 for better determination of the charge-sensing parameters.

One limitation of this model deserves particular attention. A resonance in the channel makes conductance away from a dot resonance nonlinear on the scale of V_s , while the model assumes linearity. Thus, while the model trivially fits Fig. 2(a) with $g_{coh} = 0$, it cannot account for Fig. 3 in this manner. However, the asymmetric line shapes in Fig. 3 do give somewhat plausible fits. To unambiguously identify a Fano resonance, it is necessary that the off-resonant conductance varies linearly, in turn requiring resonances to be well separated so that background behavior can be isolated.

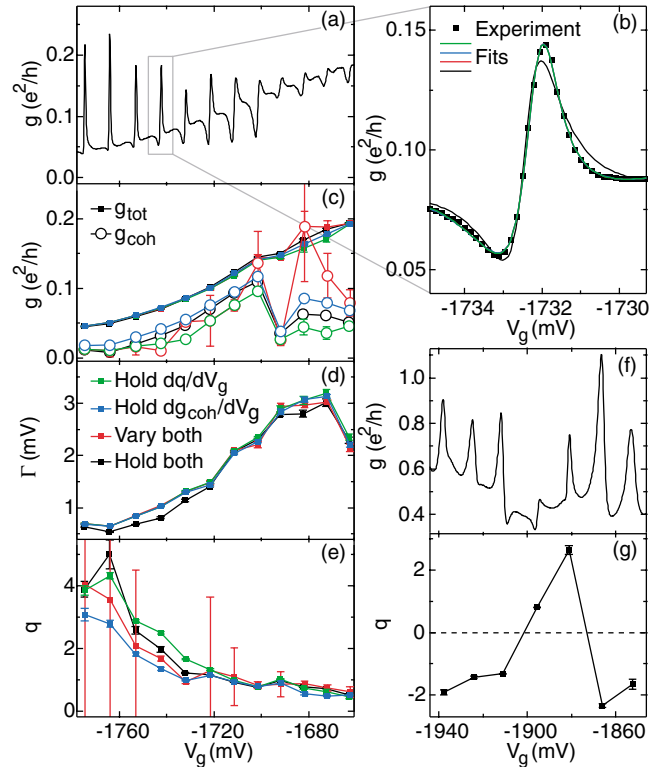


FIG. 4 (color). (a) Experimental data with 12 Fano resonances. In (b) we show one resonance and its four fits. The fits fix both (black), one (green, blue), or neither (red) of the parameters dq/dV_g and dg_{coh}/dV_g at zero. All four are shown, but the latter three are indistinguishable. In (c)-(e) we plot g_{tot} and g_{coh} , Γ , and q from (a), using the same colors to denote fitting method. Panel (f) shows data exhibiting reversals of q , with extracted q values shown in (g).

Figure 4 shows fits and the information this yields. Each resonance in Fig. 4(a) was fit four times, using all permutations of varying or zeroing dq/dV_g and dg_{coh}/dV_g , to investigate whether this unusual sensing is necessary to explain the data. Results for one resonance are shown in Fig. 4(b). The first fit holds both at zero while dg_{tot}/dV_g , V_s , and the five parameters of a basic Fano resonance are varied. This reproduces all features qualitatively, but quantitative agreement is much poorer than in the latter three fits, which are nearly identical and match experiment to almost within the noise [15]. We therefore conclude that at least one of q and g_{coh} is subject to charge sensing, implying that the potential felt by the charge in resonance is modified by its own probability to be in the dot.

Finally, we consider parameter correlations among subsequent resonances. Figs. 4(c)–4(e) show g_{tot} and g_{coh} , Γ , and q extracted from each fit to each resonance in Fig. 4(a). Most trends are consistent with general arguments about tunneling wave functions: as g_{tot} increases, indicating lower channel potential, Γ increases due to a lower tunnel barrier, and q decreases to keep peak conductance, $g_{inc} + g_{coh}(q^2 + 1)$, relatively constant. On top of this there appear to be fluctuations in g_{coh} , Γ , and q which are expected as subsequent dot wave functions have different amplitudes near the barrier.

Two other features stand out in the data. First, the fractional coherence g_{coh}/g_{tot} is often roughly constant for several peaks then jumps abruptly to a different level for subsequent peaks, as in Fig. 4 at $V_g = -1700$ mV, while g_{tot} and other parameters evolve smoothly. Observed coherence ranges from $<10\%$ to $>50\%$ [16], likely due to multiple channel modes coupling differently to the dot. Jumps in g_{coh}/g_{tot} may reflect abrupt rearrangement of dot wave functions, changing its coupling to each channel mode while total coupling Γ is nearly unchanged.

Second, changes to the sign of q are present but infrequent. An example is shown in Figs. 4(f) and 4(g), where q flips twice. Previous observations of mesoscopic Fano resonance in transmission [3], including a dot in an Aharonov-Bohm ring [17], showed a constant sign of q , sparking debate on why no reversals were seen when simple theory predicts that consecutive peaks always change sign [14,18]. In the present geometry, however, as with recent work on Fano resonance in reflection [4], uniform sign is expected as the resonance involves only one lead, leaving no relative sign between two matrix elements to reverse the phase. Why, then, are different signs of q observed here at all? One possibility is that the scattering phase in the channel changes by π , as if it too passed through a resonance [19]. This requires q to pass smoothly through zero at a maximum g_{tot} , consistent with the observation that q is mostly positive in some regions and negative in others, but this cannot explain the flips in Fig. 4(f). A more likely explanation is that the

source and drain leads couple to slightly different locations in the dot. With appropriate nodes in several wave functions, the source and drain couplings have opposite signs and q reverses for several resonances, exactly as in Fig. 4(f). In short, both coherence jumps and Fano parameter flips can be explained by imperfect one-dimensionality of the channel and the tunnel barrier.

We thank A. A. Clerk, W. Hofstetter, and B. I. Halperin for useful discussion and N. J. Craig for experimental contributions. This work was supported in part by the ARO under Grant No. DAAD19-99-1-0215 and the Harvard NSF-NSEC (Grant No. PHY-0117795). A. C. J. acknowledges support from the NSF.

-
- [1] U. Fano, Phys. Rev. **124**, 1866 (1961).
 - [2] V. Madhavan *et al.*, Science **280**, 567 (1998).
 - [3] J. Gores *et al.*, Phys. Rev. B **62**, 2188 (2000); I. G. Zacharia *et al.*, Phys. Rev. B **64**, 155311 (2001); C. Fuhner *et al.*, cond-mat/0307590; K. Kobayashi *et al.*, Phys. Rev. Lett. **88**, 256806 (2002).
 - [4] K. Kobayashi *et al.*, Phys. Rev. B **70**, 035319 (2004).
 - [5] J. Kim *et al.*, Phys. Rev. Lett. **90**, 166403 (2003).
 - [6] A. A. Clerk, X. Waintal, and P.W. Brouwer, Phys. Rev. Lett. **86**, 4636 (2001).
 - [7] Y.-J. Xiong and S.-J. Xiong, Int. J. Mod. Phys. B **16**, 1479 (2002).
 - [8] J. F. Song, Y. Ochiai, and J. P. Bird, Appl. Phys. Lett. **82**, 4561 (2003).
 - [9] M. Field *et al.*, Phys. Rev. Lett. **70**, 1311 (1993); I. Amlani *et al.*, Appl. Phys. Lett. **71**, 1730 (1997); D. S. Duncan *et al.*, Appl. Phys. Lett. **74**, 1045 (1999).
 - [10] I. H. Chan *et al.*, Appl. Phys. Lett. **80**, 1818 (2002); I. H. Chan *et al.*, Physica E (Amsterdam) **17**, 584 (2003).
 - [11] G. Breit and E. Wigner, Phys. Rev. **49**, 519 (1936).
 - [12] Adding amplitudes is an approximation which inflates extracted coherence for poorly-separated resonances. Avoiding this requires choosing a microscopic model. See A. Aharony *et al.*, Phys. Rev. B **66**, 115311 (2002).
 - [13] T. K. Ng and P. A. Lee, Phys. Rev. Lett. **61**, 1768 (1988).
 - [14] T. Taniguchi and M. Buttiker, Phys. Rev. B **60**, 13814 (1999).
 - [15] In some cases all four fits are distinct, but near-degeneracy is typical. Therefore, the fit is unreliable when both parameters are varied, hence the erratic behavior and large error bars on the parameters in red.
 - [16] This is a conservative bound from the ratio of g_{min} to g_{tot} . Extracted g_{coh}/g_{tot} reaches 90%, because charge sensing raises g_{min} even if $g_{inc} = 0$.
 - [17] A. Yacoby *et al.*, Phys. Rev. Lett. **74**, 4047 (1995); R. Schuster *et al.*, Nature (London) **385**, 417 (1997).
 - [18] R. Baltin and Y. Gefen, Phys. Rev. Lett. **83**, 5094 (1999); A. Levy Yeyati and M. Buttiker, Phys. Rev. B **62**, 7307 (2000); H. Q. Xu and B.-Y. Gu, J. Phys. Condens. Matter **13**, 3599 (2001); T.-S. Kim and S. Hershfield, Phys. Rev. B **67**, 235330 (2003).
 - [19] A. A. Clerk (private communication).